

# A library of high resolution Kurucz spectra in the wavelength range 3000 – 10000 Å

T. Murphy<sup>\*†</sup>, A. Meiksin

*Institute for Astronomy, University of Edinburgh, Royal Observatory, Blackford Hill, Edinburgh, EH9 3HJ*

Released 2002 Xxxxx XX

## ABSTRACT

We present a library of 6410 synthetic spectra with resolution  $\lambda/\Delta\lambda = 250\,000$  based on the revised Kurucz 1993 model atmospheres. The library covers the wavelength range 3000–10 000 Å with 54 values of effective temperature in the range 5250–50 000 K, 11 values of log surface gravity between 0.0 and 5.0 and 19 metallicities in the range –5.0 to 1.0. We find that, with a few caveats, the library compares well with both the original 20 Å Kurucz spectra and also with observed spectra. The library is intended for use in population synthesis and physical parameterisation of stellar spectra. We assess the suitability of the library for these tasks.

**Key words:** stars – atmospheres

## 1 INTRODUCTION

Progress in population synthesis and automatic classification of stellar spectra has been limited by the spectral resolution of the available synthetic stellar spectra. The existing synthetic libraries are not at high enough resolution to be useful for classifying stars from recent surveys such as the SDSS (Stoughton et al. 2002) ( $\lambda/\Delta\lambda \sim 1800$ ), or future surveys such as RAVE (Steinmetz 2002) and GAIA (Lindgren & Perryman 1996). Most classification techniques smooth the observed spectra to the resolution of the synthetic spectra. This means much of the detailed information in the observed spectra is lost, which may reduce the quality of the classifications. Population synthesis packages such as PEGASE (Fioc & Rocca-Volmerange 1997) or GISSEL (Bruzual A. & Charlot 1993) use a grid of stellar spectra to generate galaxy spectra. The resulting galaxy spectra are limited by the resolution of the input stellar spectra. To study the high resolution features, it is necessary to have a grid of observed or synthetic stellar spectra which match the resolution of the observed galaxy spectra. For example, galaxy spectra synthesised from 20 Å spectra cannot be used to measure standard line indices like the Lick indices.

Perhaps the most widely used library of synthetic spectra are the flux distributions from the Kurucz ATLAS9 model atmospheres (Kurucz 1993a). It is important to note that while these are usually referred to as spectra, they are flux distributions predicted directly from the model atmo-

spheres, rather than spectra generated by a spectral synthesis program. The Kurucz atmospheres have several disadvantages which are discussed in various sources such as Kurucz (1992). However, one of their advantages is the wide range of parameters they cover, which is important for generating a grid of stellar spectra for population synthesis. The need for higher resolution spectra has been recognised for some time but, because of the immense computational expense involved, the synthesis of the spectra has been limited to partial wavelength ranges and specific regions of parameter space. Several groups have generated libraries of spectra from the Kurucz model atmospheres. For example, Chavez, Malagnini, & Morossi (1997) provide a set of 711 Kurucz spectra at  $\lambda/\Delta\lambda = 250\,000$  in the wavelength region 4850–5400 Å and Castelli & Munari (2001) have generated a set of 698 Kurucz spectra at  $\lambda/\Delta\lambda = 20\,000$ , in the wavelength region 7650–8750 Å for use with GAIA spectra. González Delgado & Leitherer (1999) have generated synthetic spectra in very small spectra regions necessary for a particular application. They created a grid of synthetic profiles of stellar H Balmer and HeI lines at  $\Delta\lambda = 0.3$  Å for the purposes of evolutionary synthesis.

There are also several libraries of observed spectra now available at much higher resolution. For example, the ELODIE database (Prugniel & Soubiran 2001), consists of 709 stars observed in the wavelength range 4100–6800 Å with a resolution of  $\lambda/\Delta\lambda \sim 42\,000$ . STELIB (Le Borgne et al. 2003) provides spectra for 249 stars observed in the wavelength range 3200–9500 Å with a resolution of  $\lambda/\Delta\lambda \sim 2000$ . The observed libraries are crucial for evaluating the accuracy of synthetic spectra and can also be used directly for population synthesis and classification. STELIB has been used by Kauffmann et al. (2003) with a new version of GISSEL,

\* Present address: Australia Telescope National Facility, CSIRO, P.O. Box 76, Epping, NSW 1710, Australia

† Email: Tara.Murphy@csiro.au

and ELODIE has been used to assign physical parameters to stars observed by the SDSS. However, a limitation of the observed spectral libraries is that they do not cover the full range in parameter space needed for galaxy population synthesis. Complete coverage of the parameter space is even more important for stellar spectral classification. The most successful approaches to classification have used methods from machine learning (Bailer-Jones 2001). In these methods, the distribution of spectra in the training set has a direct impact on the accuracy of the classification assigned to new spectra.

There are several efforts to generate higher resolution Kurucz spectra that are currently in progress. Bertone et al. (2002) have generated a grid of 832 spectra at  $\lambda/\Delta\lambda = 500\,000$  over the wavelength range 3500 – 7000 Å. They intend to extend the wavelength range down to 850 Å at a resolution of  $\lambda/\Delta\lambda = 50\,000$ . Zwitter, Munari, & Castelli (2002) are in the process of generating a grid of Kurucz spectra at  $\lambda/\Delta\lambda = 20\,000$  over the wavelength range 2500 – 10 500 Å for use in radial velocity correction work.

We have generated a larger library of 6410 spectra from the Kurucz model atmospheres. Previously these spectra were only available either at much lower resolution (20 Å) or over small wavelength ranges. Our spectra were generated from ATLAS9 model atmospheres, using John Lester’s Unix version of the SYNTHE spectral synthesis package (Lester 2002, private communication). We have modified this package to improve the efficiency of the code, making it possible to generate the complete range of Kurucz spectra in a reasonable time.

This paper compares our higher resolution spectra with the original 20 Å Kurucz spectra and the STELIB library of observed spectra. In Section 2 we describe the main characteristics of the new library of spectra. In Section 3 we compare the spectra with the 20 Å Kurucz spectra from Kurucz (1993a). Finally, in Section 4 we compare the spectra with observed spectra from the STELIB library. We will make this library of spectra available for general use on request.

## 2 GENERATING THE KURUCZ SPECTRA

The library presented here has been created using the updated versions of the ATLAS9 model atmospheres from Kurucz (1993a). These are available from Kurucz’s website (labelled `.dat`). Kurucz advises that the Kurucz (1993a) models (labelled `.datCD`) should not be used as they have a discontinuity in the fluxes and colours as a function of  $T_{\text{eff}}$  and  $\log(g)$  that was corrected for the revised version.

The models assume plane parallel homogeneous layers in steady-state, local thermal equilibrium. A microturbulence velocity of 2  $\text{kms}^{-1}$  and a mixing-length value of  $\ell/H_p = 1.25$  are used. Castelli, Gratton, & Kurucz (1997) give a detailed discussion of whether the mixing length theory for convection is dealt with adequately in the standard Kurucz atmospheres. They have calculated an alternative set of atmospheres in which the Kurucz “overshooting” approximation is not used (NOVER models). These models have been shown to predict more accurate observable properties (eg. colours) for some atmospheres ((Heiter et al. 2002; Smalley & Kupka 1997; Smalley et al. 2002)). However, since they are currently available only for some metal-

licity values (-2.5, -2.0, -1.5, -1.0, -0.5, 0.0, +0.5 dex) we decided not to use these atmospheres for population synthesis. We have generated a small subset of the NOVER models for comparison with the STELIB spectra.

The adopted atomic line lists for all our spectra are LOWLINES and NLTE LINES from Kurucz (1994) and the adopted molecular line list is DIATOMIC from Kurucz (1993b). We have included both predicted and measured lines. The inclusion of the predicted lines is necessary to reproduce accurate flux distributions. However, it does mean that care should be taken when using the high resolution spectra, as the properties of individual lines may not be as accurate as if Kurucz’s more up to date line lists (which do not include predicted lines) were used. The molecular lines have been included for spectra with  $T_{\text{eff}} \leq 7000$  K.

The original programs making up the Kurucz package were written in FORTRAN77 for the VAX. John Lester has written a Unix version based on the original Kurucz code, in FORTRAN77 and a more recent Unix version in Fortran90 (Lester 2002, private communication). However, this code could only be used to generate small sections of a spectrum at a time because it required massive quantities of disk space. The complexities in generating spectra with SYNTHE has restricted researchers to creating either a small number of spectra, or a large number over a very small wavelength range. We have modified the Lester code to dramatically reduce the disk usage of SYNTHE which makes it feasible to generate large spectral ranges on standard hardware in a relatively short period of time. We have not yet generated spectra for values of  $T_{\text{eff}} \leq 5000$  K. These spectra require TiO lines to be included which makes the program significantly slower, and requires more disk space and we are investigating whether further optimisations may be made.

One thing to note is the subtle difference in terminology between ‘spectra’ and ‘flux distributions’ which are sometimes used interchangeably. The Kurucz 20 Å flux distributions were predicted directly from the Kurucz model atmospheres. The ATLAS9 model atmosphere program sums up the opacity in broad 10 or 20 Å bins creating a low resolution spectrum. The Kurucz spectra that we have generated have been calculated from the model atmospheres, using the SYNTHE software. These spectra are generated at extremely high resolution (ideally as high as the computational resources allow) and then rebinned to the required resolution. The newest versions of ATLAS9 will combine both the model atmosphere generation and the spectral synthesis into one process.

Of the 7216 model atmospheres available in Kurucz’s standard distribution, we have generated a grid of 6410 spectra, which excludes the lowest temperature spectra. The spectra cover the wavelength range 3000 – 10 000 Å which was chosen to be useful for comparisons with SDSS spectra. The spectra were generated at a resolution of  $\lambda/\Delta\lambda = 250\,000$ .

## 3 COMPARISONS WITH THE 20Å KURUCZ SPECTRA

In this section we compare our library of spectra with the revised version of the 20 Å Kurucz flux distributions. There have been several changes to the software and data between

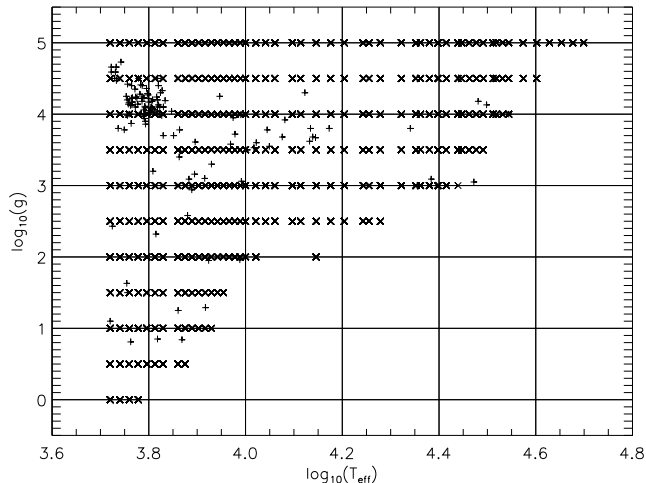


**Figure 1.** The distribution of our Kurucz spectra in  $\log(T_{\text{eff}}) - \log(g)$  space ( $\times$ ). Also plotted is the distribution of the STELIB spectra with  $T_{\text{eff}} > 5000$  K ( $+$ ).

the original release of the  $20 \text{ \AA}$  Kurucz flux distributions, and the present. Also, the flux distributions are predicted directly from the model atmosphere code, so it is not possible to compare them directly with the spectra generated by spectral synthesis. Because of this, the spectra we have generated are not expected to match the flux distributions exactly, but it is an important check to make sure there was broad agreement between the spectra.

### 3.1 Direct comparisons

We compare the higher resolution Kurucz spectra with the  $20 \text{ \AA}$  flux distributions. Figure 2 shows several examples of these comparisons. For the purposes of this comparison, we re-binned the new spectra to  $20 \text{ \AA}$  using a simple top-hat function. There are several differences between the two sets of spectra:

(i) In all the spectra there is an extra dip in the new spectra at around  $3700 \text{ \AA}$ . This is due to inadequate treatment of the Balmer jump. In the model atmosphere code, the way the Balmer jump is dealt with has been modified in order to remove the dip (Kurucz, private communication).

(ii) In some of the lower temperature spectra, the shape of the Ca H/K doublet is not identical. This is largely due to the fact that for the model atmospheres, the Stark broadening was artificially increased to make up for missing lines in computing the distribution function (Kurucz, private communication). This was changed back to generate the synthetic spectra, and also for more recent flux distributions.

(iii) In lower temperature spectra ( $T_{\text{eff}} \leq 7000$  K) there is a systematic difference in flux in the G-band. This is likely to be due to changes in the molecular line lists since the flux distributions were produced.

(iv) Most of the strong lines have slightly different depths. These small peaks are likely to be unresolved line cores, caused by the fact that the  $20 \text{ \AA}$  flux distributions are under-sampled, whereas our new synthetic spectra are generated at high resolution.

Probably the most significant of these points for our applications is the difference in the G-band flux. This affects individual lines, and the  $U$  band magnitude of the spectra. In the following sections we quantify this.

### 3.2 Colours

Comparing the  $UBVRI$  magnitudes is important for checking that the broadband properties of the spectra are reproduced. We have used the Johnson-Cousins bandpasses, as defined by Bessell (1990). Figure 3 shows the offset in magnitudes calculated for the new spectra and the  $20 \text{ \AA}$  flux distributions. The RMS errors for the colours for the two sets of spectra are:  $\Delta U = 0.05$  mag,  $\Delta B = 0.01$  mag,  $\Delta V = 0.01$  mag,  $\Delta R = 0.01$  mag and  $\Delta I = 0.01$  mag. The  $B$ ,  $V$ ,  $R$  and  $I$  magnitudes are in good agreement. However, the differences are greater for the  $U$  magnitudes at lower temperatures ( $T_{\text{eff}} \leq 7000$  K). For higher temperature spectra the  $U$  magnitudes are also in good agreement. The  $U$  band discrepancy is probably a consequence of the differences in the spectra noted in Section 3.1.

The question is how important these magnitude offsets are for the applications we are interested in. A difference in measured colour is largely degenerate with a difference in  $T_{\text{eff}}$ . For example, Lejeune, Cuisinier, & Buser (1997) find that the colour vs. temperature relations for Kurucz spectra do not match those derived empirically. To fix the problem, they developed a method for adjusting the shape of the continuum (in other words change the magnitudes) for spectra of a certain  $T_{\text{eff}}$ . However, an alternative approach is to leave the shape of the spectrum unchanged and re-assign a  $T_{\text{eff}}$  to the spectrum. For example, a solar metallicity spectrum with  $T_{\text{eff}} = 7500$  and  $\log(g) = 1.0$  has a  $U$  magnitude offset of 0.05. This difference in colour between our new spectrum and the Kurucz flux distribution corresponds to a change of  $T_{\text{eff}}$  by less than 30 K. Since quoted errors for temperatures on observed spectra are typically around 40 – 100 K (see for example Katz et al. (1998) or Alonso, Arribas, & Martínez-Roger (1999)), the spectra agree to within usual measurement errors.

## 4 COMPARISONS WITH OBSERVED SPECTRA

Having shown that the new spectra agree reasonably well with the  $20 \text{ \AA}$  flux distributions, the next step is to evaluate them against observed spectra. This serves two purposes. Firstly, there are some differences between the two sets of Kurucz spectra, especially in the blue. However, if these differences are smaller than the differences between one of the Kurucz spectra and an observed spectrum with the same physical parameters, then they may be neglected. Secondly, we want to evaluate what kind of applications the synthetic spectra can be used for. Our aim is to demonstrate that our new Kurucz spectra are as suitable for use in population synthesis as the commonly used  $20 \text{ \AA}$  Kurucz flux distributions, but with the advantage of higher resolution. There are already various comparisons of Kurucz spectra with observed spectra in the literature. For example, the colour– $T_{\text{eff}}$  correlation for the spectra has been analysed by Lejeune et al. (1997) and the  $20 \text{ \AA}$  spectra have been compared with

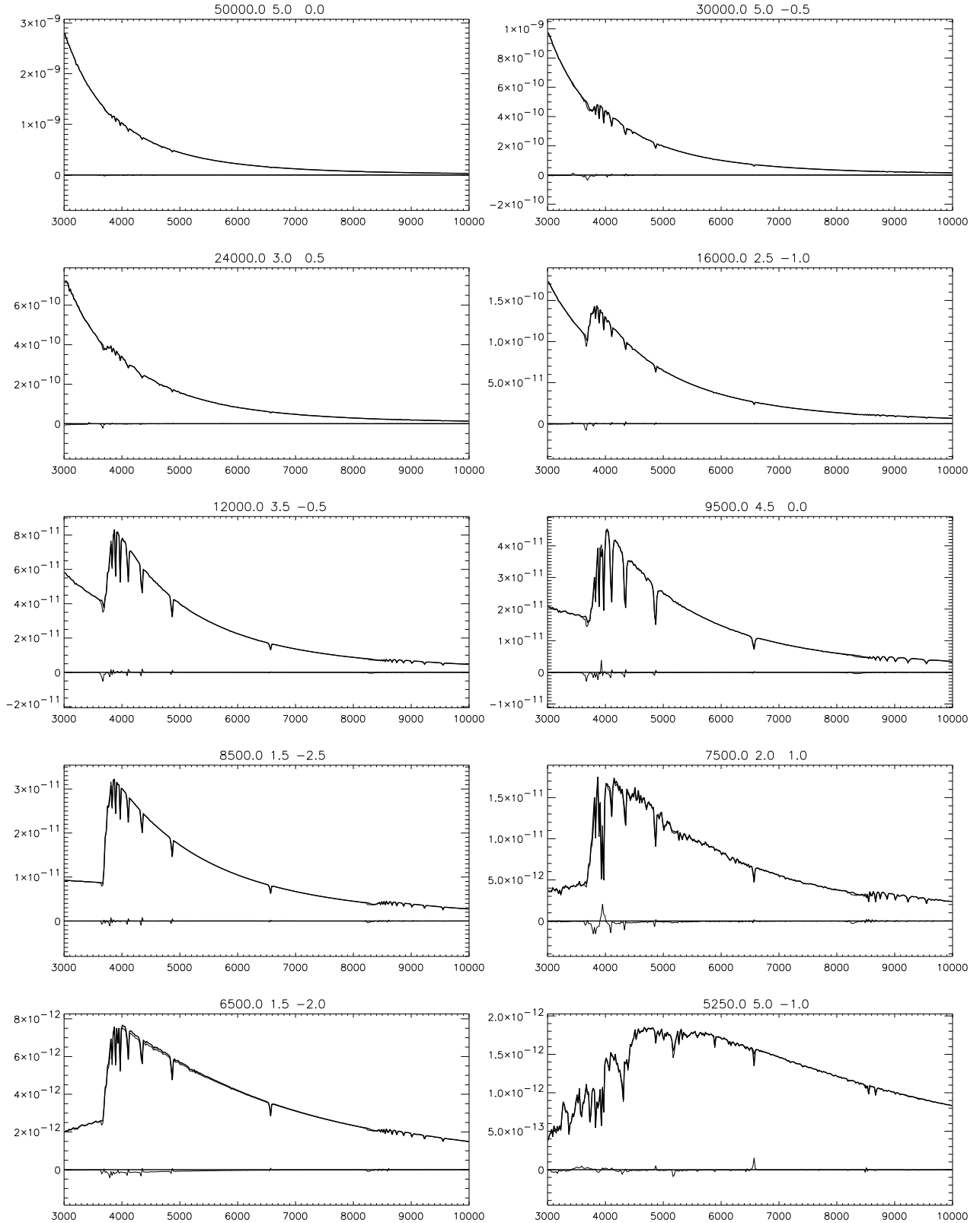


**Figure 2.** Comparison between a sample of the  $20 \text{ \AA}$  Kurucz flux distributions (bold line) and the newly generated Kurucz spectra (thin line) (box-car smoothed to  $\Delta\lambda = 20\text{\AA}$ ). These spectra cover a range of physical parameters: the title of each plot gives the values for  $T_{\text{eff}}$ ,  $\log(g)$  and  $[Fe/H]$ . The x-axis is the wavelength in  $\text{\AA}$  and the y-axis is flux,  $F(\lambda)$ , in arbitrary units. Underneath each pair of spectra is  $\Delta F = F(\lambda)_{\text{new}} - F(\lambda)_{\text{old}}$ .

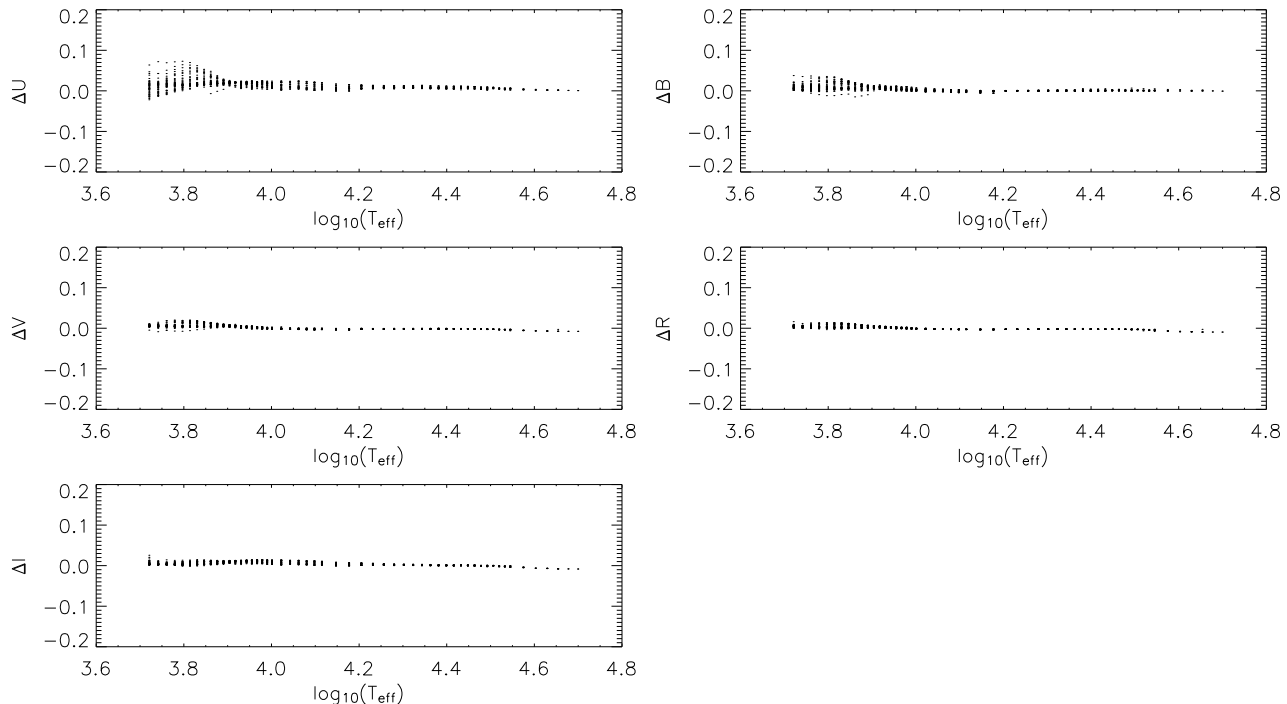


**Figure 3.** Magnitude offsets between our Kurucz spectra and the 20 Å flux distributions. The x-axis is  $\log_{10}(T_{\text{eff}})$  and the y-axis shows the difference (in magnitudes) between the Kurucz spectra we have generated and the 20 Å flux distributions.

observed spectra by Straižys, Liubertas, & Valiauga (1997) and Straižys, Lazauskaite, & Valiauga (2002). We here make our own comparisons to focus on properties such as the Lick indices which are relevant to the specific applications we are interested in.

We have compared the spectra to those in the STELIB library (Le Borgne et al. 2003), which consists of 250 spectra in the visible range (3200–9500 Å) with a spectral resolution of  $\Delta\lambda \lesssim 3$  Å and covering a wide range in parameter space. As well as a direct comparison of the SEDs, we compare the measured colours and Lick indices to confirm that the spectra meet our requirements.

Many of the STELIB stars do not have values for all three physical parameters ( $T_{\text{eff}}$ ,  $\log(g)$  and  $[Fe/H]$ ), have large sections of the spectrum missing, or do not lie close to a point on our grid of spectra. Hence we have selected a subset of 125 of the spectra that have tabulated values for  $T_{\text{eff}}$ ,  $\log(g)$  and  $[Fe/H]$  in Le Borgne et al. (2003),  $T_{\text{eff}} > 5000\text{K}$ , and which have a good  $\chi^2$  match to the corresponding Kurucz spectrum. The values for most of the physical parameters were obtained from the Cayrel de Strobel et al. (1997) and Cayrel de Strobel, Soubiran, & Ralite (2001) catalogues. However, some were obtained from the ELODIE database (Prugniel & Soubiran 2001) and several were calculated using the TGMET method (Katz et al. 1998). We corrected the spectra for interstellar reddening using the values of  $A_V$  from Le Borgne et al. (2003) and the IDL ASTROLIB routine CCM\_DERED.PRO. The STELIB spectra have not been corrected for atmospheric absorption, so they have strong absorption features (most noticeably in the Oxygen A-band around 7600Å) which are not present in the synthetic spectra.

#### 4.1 Colours

We have calculated colours for all of the STELIB spectra and their closest Kurucz matches. Since the wavelength range of the STELIB spectra is 3200 – 9500 Å, we have calculated a modified  $U$  band magnitude (denoted  $U^*$ ), which is truncated at 3200 Å for both the STELIB and Kurucz spectra. Figure 4 shows the magnitude offsets between the STELIB spectra and their Kurucz matches. The RMS error between the two sets of spectra are:  $\Delta U^* = 0.14$  mag,  $\Delta B = 0.05$  mag,  $\Delta V = 0.02$  mag,  $\Delta R = 0.03$  mag and  $\Delta I = 0.04$  mag. For comparison, we also calculated the magnitude offsets for the STELIB spectra and their closest Kurucz matches, using the 20 Å flux distributions. The RMS error between these two sets of spectra are:  $\Delta U^* = 0.11$  mag,  $\Delta B = 0.05$  mag,  $\Delta V = 0.02$  mag,  $\Delta R = 0.03$  mag and  $\Delta I = 0.04$  mag. This demonstrates that, with the exception of  $U^*$ , the scatter in the magnitudes is no worse for our new spectra than for the 20 Å spectra that are in standard use.

Some differences are expected due to the mismatch between the STELIB temperatures and those of the closest Kurucz match – many of the spectra have a difference in temperature of about 100 K, corresponding to a difference of a few hundredths in magnitude. However, the important point for our work is that our new spectra are as well matched to the observed spectra as the 20 Å spectra that are often used for population synthesis. Figure 5 shows various colour comparisons. There is some scatter in each of the plots and a slight systematic offset in  $R - I$ . Again however, this is no worse than when comparing the 20 Å spectra with the STELIB spectra.

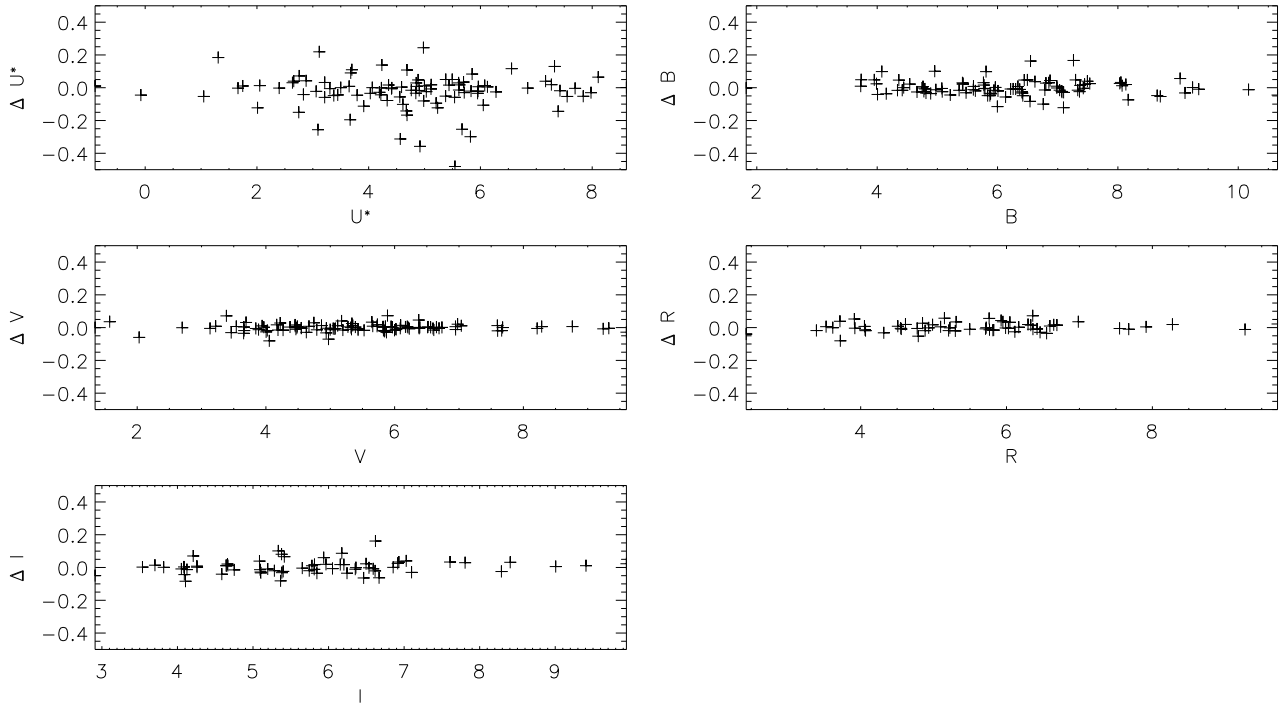


**Figure 4.** Magnitude offsets between the STELIB spectra and the closest Kurucz spectrum match from the grid.

## 4.2 Line indices

We have calculated Lick indices for each of the 125 STELIB spectra in our sample, and for the matching Kurucz spectra. There are two types of index, atomic ( $I_a$ ) and molecular ( $I_m$ ) which we have calculated from the standard formulae:

$$I_a \equiv \int_{\lambda_{c1}}^{\lambda_{c2}} \left[ 1 - \frac{S(\lambda)}{C(\lambda)} \right] d\lambda \quad (1)$$

$$I_m \equiv -2.5 \log_{10} \frac{\int_{\lambda_{c1}}^{\lambda_{c2}} \frac{S(\lambda)}{C(\lambda)} d\lambda}{\lambda_{c2} - \lambda_{c1}} \quad (2)$$

where  $\lambda_{c1}$  and  $\lambda_{c2}$  are the limits of the central bandpass defining the index (in Å),  $S(\lambda)$  is the object spectrum and  $C(\lambda)$  is the linearly interpolated pseudo-continuum, defined by

$$C(\lambda) \equiv S_b \frac{\lambda_r - \lambda}{\lambda_r - \lambda_b} + S_r \frac{\lambda - \lambda_b}{\lambda_r - \lambda_b}. \quad (3)$$

Here,

$$S_b \equiv \frac{\int_{\lambda_{b1}}^{\lambda_{b2}} S(\lambda) d\lambda}{\lambda_{b2} - \lambda_{b1}}, \quad \lambda_b \equiv (\lambda_{b1} + \lambda_{b2})/2 \quad (4)$$

$$S_r \equiv \frac{\int_{\lambda_{r1}}^{\lambda_{r2}} S(\lambda) d\lambda}{\lambda_{r2} - \lambda_{r1}}, \quad \lambda_r \equiv (\lambda_{r1} + \lambda_{r2})/2 \quad (5)$$

and  $\lambda_{b1}$ ,  $\lambda_{b2}$ ,  $\lambda_{r1}$  and  $\lambda_{r2}$  are the limits of the blue and red continuum bands. The bandpass definitions for the Lick indices and the red and blue pseudo-continua are those defined in Worthey et al. (1994). These are given in Table 1.

A method for random error estimation in line-strength indices is outlined in detail by Cardiel et al. (1998). The resulting equations are based on a full analysis of the error propagation throughout the calculation process. The result-

ing random errors are given by:

$$\sigma^2[I_a] = \sum_{i=1}^{N_{\text{pixels}}} \left[ \frac{C^2(\lambda_i) \sigma^2(\lambda_i) + S^2(\lambda_i) \sigma_{C(\lambda_i)}^2}{C^4(\lambda_i)} \right] d\lambda_i^2 + \sum_{i=1}^{N_{\text{pixels}}} \sum_{j=1, j \neq i}^{N_{\text{pixels}}} \left[ \frac{S(\lambda_i) S(\lambda_j)}{C^2(\lambda_i) C^2(\lambda_j)} (\Lambda_1 \sigma_{S_b}^2 + \Lambda_4 \sigma_{S_r}^2) \right] d\lambda_i d\lambda_j \quad (6)$$

for the atomic indices and:

$$\sigma[I_m] = 2.5 \frac{\log(e)}{10^{-0.4 I_m}} \frac{1}{\lambda_{c2} - \lambda_{c1}} \sigma[I_a] \quad (7)$$

for the molecular indices, where

$$\Lambda_1 \equiv \frac{(\lambda_r - \lambda_i)(\lambda_r - \lambda_j)}{(\lambda_r - \lambda_b)^2} \quad (8)$$

$$\Lambda_4 \equiv \frac{(\lambda_i - \lambda_b)(\lambda_j - \lambda_b)}{(\lambda_r - \lambda_b)^2} \quad (9)$$

$$\sigma_{C(\lambda_i)}^2 = \left( \frac{\lambda_r - \lambda_i}{\lambda_r - \lambda_b} \right) \sigma_{S_b}^2 + \left( \frac{\lambda_i - \lambda_b}{\lambda_r - \lambda_b} \right) \sigma_{S_r}^2 \quad (10)$$

$$\sigma_{S_b}^2 = \frac{1}{(\lambda_{b2} - \lambda_{b1})^2} \sum_{i=1}^{N_{\text{pixels}}(\text{blue})} \sigma^2(\lambda_i) d\lambda_i^2 \quad (11)$$

$$\sigma_{S_r}^2 = \frac{1}{(\lambda_{r2} - \lambda_{r1})^2} \sum_{i=1}^{N_{\text{pixels}}(\text{red})} \sigma^2(\lambda_i) d\lambda_i^2. \quad (12)$$

Note that Cardiel et al. (1998) assume the size of each pixel  $d\lambda$  ( $\Theta$  in their notation) is fixed, and so take it out of all the summations. However, in general (and in our case),  $d\lambda$  is not fixed, and so we keep it inside the summation signs.

Figure 6 shows the correlation between the Lick indices calculated from the STELIB spectra and the Kurucz spectra. We have not calculated the two TiO indices since TiO

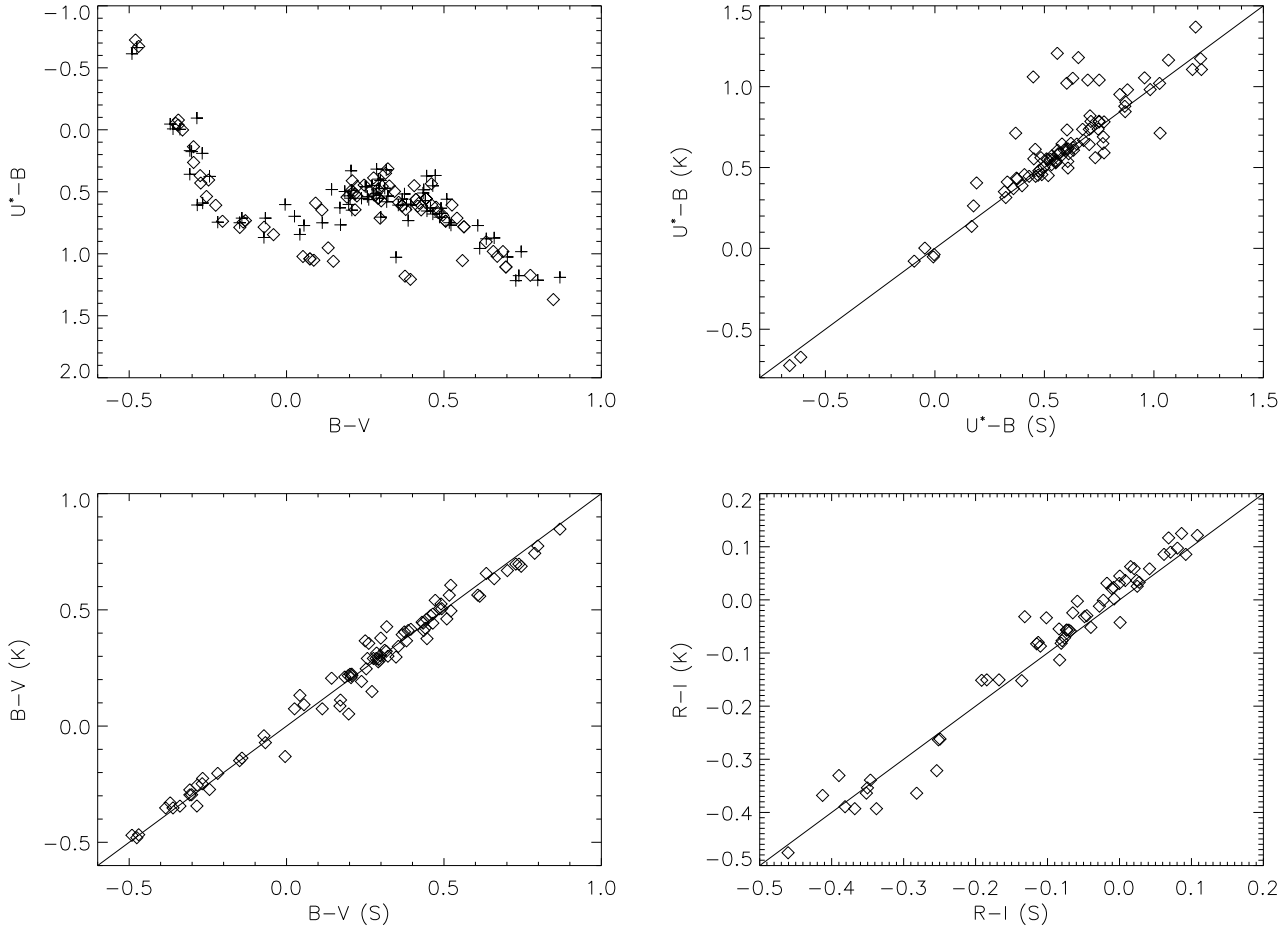


**Figure 5.** Top Left:  $U^* - B$  vs.  $B - V$  for STELIB spectra (+) and their Kurucz matches ( $\diamond$ ). Top Right:  $U^* - B$  colours for STELIB spectra ( $x$ -axis) and their Kurucz matches ( $y$ -axis). The solid line is the line “ $x = y$ ” for comparison. Bottom Left: Comparison of  $B - V$  colours. Bottom Right: Comparison of  $R - I$  colours.

Name	Central Bandpass	Blue Continuum	Red Continuum	Type
CN <sub>1</sub>	4142.125 – 4177.125	4080.125 – 4117.625	4244.125 – 4284.125	M
CN <sub>2</sub>	4142.125 – 4177.125	4083.875 – 4096.375	4244.125 – 4284.125	M
Ca4227	4222.250 – 4234.750	4211.000 – 4219.750	4241.000 – 4251.000	A
G4300	4281.375 – 4316.375	4266.375 – 4282.625	4318.875 – 4335.125	A
Fe4383	4369.125 – 4420.375	4359.125 – 4370.375	4442.875 – 4455.375	A
Ca4455	4452.125 – 4474.625	4445.875 – 4454.625	4477.125 – 4492.125	A
Fe4531	4514.250 – 4559.250	4504.250 – 4514.250	4560.500 – 4579.250	A
Fe4668	4634.000 – 4720.250	4611.500 – 4630.250	4742.750 – 4756.500	A
H <sub>β</sub>	4847.875 – 4876.625	4827.875 – 4847.875	4876.625 – 4891.625	A
Fe5015	4977.750 – 5054.000	4946.500 – 4977.750	5054.000 – 5065.250	A
Mg <sub>1</sub>	5069.125 – 5134.125	4895.125 – 4957.625	5301.125 – 5366.125	M
Mg <sub>2</sub>	5154.125 – 5196.625	4895.125 – 4957.625	5301.125 – 5366.125	M
Mg <sub>b</sub>	5160.125 – 5192.625	5142.625 – 5161.375	5191.375 – 5206.375	A
Fe5270	5245.650 – 5285.650	5233.150 – 5248.150	5285.650 – 5318.150	A
Fe5335	5312.125 – 5352.125	5304.625 – 5315.875	5353.375 – 5363.375	A
Fe5406	5387.500 – 5415.000	5376.250 – 5387.500	5415.000 – 5425.000	A
Fe5709	5696.625 – 5720.375	5672.875 – 5696.625	5722.875 – 5736.625	A
Fe5782	5776.625 – 5796.625	5765.375 – 5775.375	5797.875 – 5811.625	A
Na <sub>D</sub>	5876.875 – 5909.375	5860.625 – 5875.625	5922.125 – 5948.125	A

**Table 1.** Bandpass definitions for the Lick indices calculated here. Each index has a type A or M signifying atomic and molecular indices, respectively. Atomic indices are measured in Å and molecular indices are measured in magnitudes. Note that these are air wavelengths.

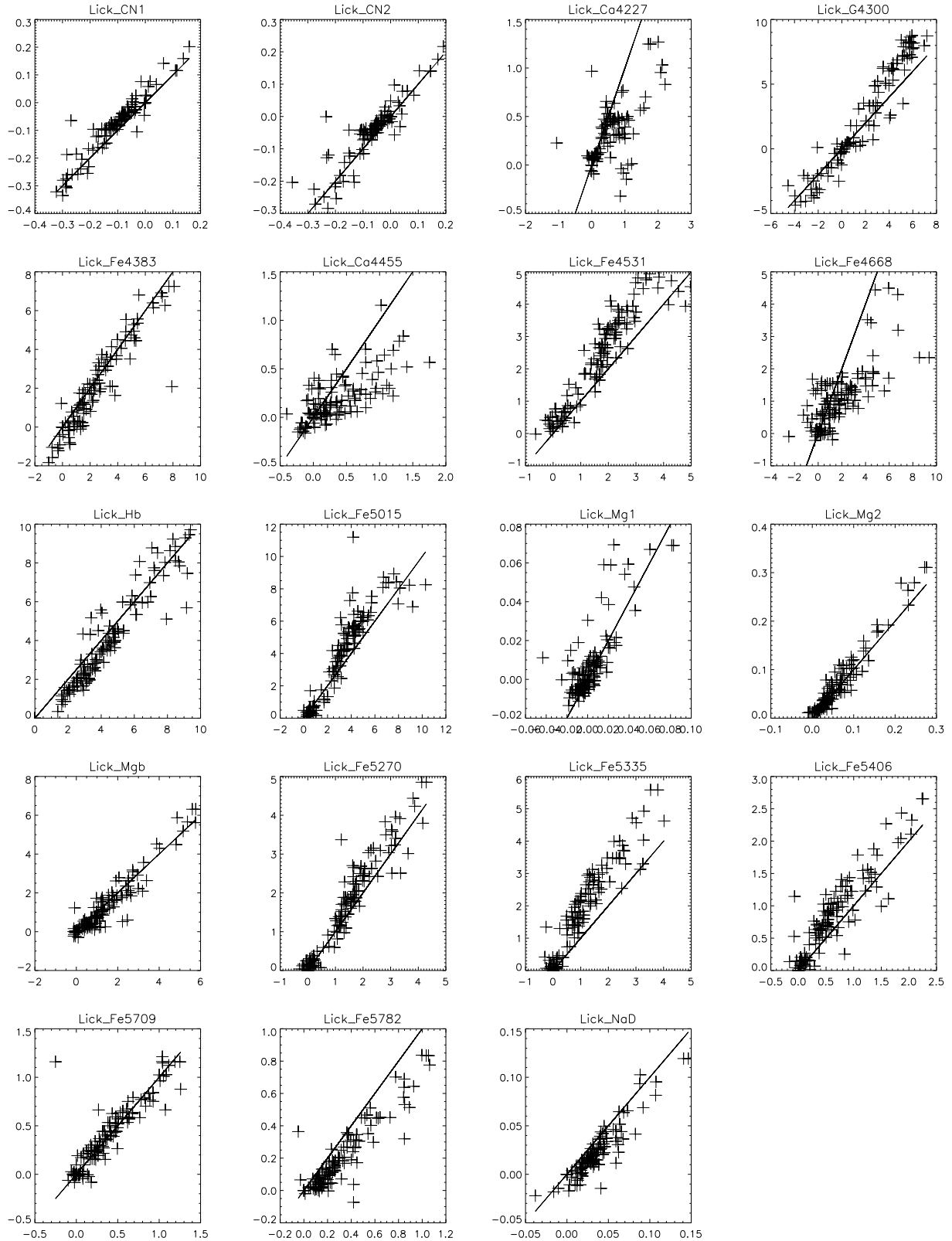


**Figure 6.** Each plot shows the correlation between the Lick index calculated on the STELIB spectrum ( $x$ -axis) and the closest matching Kurucz spectrum from our grid ( $y$ -axis). The solid line is the line “ $x = y$ ” for comparison. We have not included the TiO indices for reasons discussed in the text. The RMS error for each index is given in Table 1.

Name	Mean value	Av. Abs. Err.	Med. Abs. Err.	Type
CN <sub>1</sub>	-0.107	0.03	0.02	M
CN <sub>2</sub>	-0.066	0.03	0.01	M
Ca4227	0.583	0.33	0.03	A
G4300	2.028	1.28	0.42	A
Fe4383	2.593	0.63	0.95	A
Ca4455	0.366	0.27	0.27	A
Fe4531	1.698	0.72	0.02	A
Fe4668	1.732	1.12	2.17	A
H <sub>β</sub>	4.430	0.76	0.66	A
Fe5015	3.342	0.96	0.08	A
Mg <sub>1</sub>	0.003	0.01	0.00	M
Mg <sub>2</sub>	0.061	0.01	0.02	M
Mg <sub>b</sub>	1.430	0.33	0.07	A
Fe5270	1.493	0.34	0.02	A
Fe5335	1.123	0.82	0.18	A
Fe5406	0.640	0.27	0.58	A
Fe5709	0.377	0.09	0.26	A
Fe5782	0.323	0.13	0.49	A
Na <sub>D</sub>	0.036	0.01	0.06	M

**Table 2.** Statistical comparison between the STELIB Lick indices and those of their Kurucz matches. Column 2 shows the mean value of the STELIB index. Column 3 shows the average absolute offset between the Kurucz and STELIB indices. Column 4 shows the median absolute offset between the Kurucz and STELIB indices.

lines are switched off in these spectra. The average absolute offsets (ie:  $\sum \frac{|I_k - I_s|}{n}$ ) for the correlations are given in Table 2. It should be noted that the Kurucz spectrum paired with a given STELIB spectrum is not necessarily the best possible spectrum that could be synthesised to match the STELIB spectrum, but simply the spectrum from our grid with the closest match in physical parameters. This means it does not take into account any particular properties of the STELIB spectrum that could in principle be modelled and which may affect the line indices. However, the comparison does give an indication of the level of mismatch to be expected when comparing observed stellar spectra with a grid of synthetic spectra like ours. Such mismatches are an inevitable consequence of any automated comparisons between a grid of model spectra and the vast number of spectra being made available from large surveys like the SDSS.

We have calculated Lick indices and their associated errors for a set of 9473 SDSS galaxies from the Early Data Release (Stoughton et al. 2002). This allows us to compare the scatter between the Lick index values for the STELIB and Kurucz spectra, with the expected accuracy of the indices measured from observed galaxy spectra. We have found that the random error (as calculated by Equations 6 and 7) associated with each index measured in the SDSS spectra, is of the same order of magnitude as the average offset between the Kurucz and STELIB index measurement. This suggests that the indices measured from galaxy spectra synthesised from the Kurucz spectra will have at least comparable accuracy to those measured with SDSS, and so our grid of stellar spectra is well matched to the SDSS galaxies.

## 5 DISCUSSION

We have generated a grid of theoretical spectra from the Kurucz model atmospheres. Since the intended use of these spectra is in population synthesis and stellar classification, we have made several comparisons to check the validity of using the spectra for these purposes. The broadband properties of the spectra compare well with observed spectra, as do the line index measurements. The comparisons do not guarantee the accuracy of the Kurucz spectra as models of observed stellar spectra. Rather, they demonstrate that our new, high resolution Kurucz spectra are as good for use in population synthesis as the commonly used library of 20 Å spectra. The advantage of these spectra over the previously available Kurucz spectra is that they allow the modelling of spectral line features such as the Lick indices.

When using these spectra at high resolutions, it should be recognised that the spectra were generated using line lists that include ‘predicted’ lines. This is necessary to reproduce the broadband colours of the spectra accurately. However, it does mean that many of the individual lines present at high resolutions do not have measured properties. Also, the line lists that we used (such as LOWLINES) are known to have problems with the values for specific lines. As this mostly involves weak lines, it should not present any difficulties for population synthesis at the resolution of the SDSS. More accurate properties for these lines could be obtained using alternative values, for example from the Vienna Atomic Line Database (VALD) (Kupka et al. 2000).

Also, the 20 Å Kurucz flux distributions are often used with the corrections of Lejeune et al. (1997); Lejeune et al. (1998) applied. The corrections are an attempt to calibrate the spectra by comparing the synthetic model colours with empirical stellar colours. We investigated applying the same corrections to our high resolution spectra, but found that artifacts were introduced when using this technique directly. The Lejeune corrections mainly affect the lower temperature spectra, which we have not included in this library. For most of our spectra, the corrections are negligibly small.

We intend to extend the library to the lower temperature models in which TiO lines become important and also generate spectra for the NOVER models as these are more accurate. We are in the process of building a large library for population synthesis – a higher resolution version of that done by Lejeune et al. (1997) – which will also incorporate the NextGen models (Hauschildt, Allard, & Baron 1999a), (Hauschildt et al. 1999b).

## ACKNOWLEDGEMENTS

TM thanks the University of Edinburgh and the University of Sydney for scholarships. We would like to thank John Lester for making his code available and for the extensive help he provided in generating the spectra. We would also like to thank Ivan Baldry, Friedrich Kupka, Barry Smalley, Robert Kurucz and Ian Sheret for helpful discussions and email exchanges about various aspects of the spectra and James Curran for advice on computational issues.

## REFERENCES

- Alonso A., Arribas S., Martínez-Roger C., 1999, *A&AS*, 139, 335
- Bailer-Jones C. A. L., 2001, in Gupta R., Singh H. P., Bailer-Jones C. A. L., eds., *Automated Data Analysis in Astronomy*
- Bertone E., Buzzoni A., Rodríguez-Merino L. H., Chavez M., 2002, in Piskunov N., Weis W. W., Gray D. F., eds., *Modelling of Stellar Atmospheres*
- Bessell M. S., 1990, *PASP*, 102, 1181
- Bruzual A. G., Charlot S., 1993, *ApJ*, 405, 538
- Cardiel N., Gorgas J., Cenarro J., Gonzalez J. J., 1998, *A&AS*, 127, 597
- Castelli F., Munari U., 2001, *A&A*, 366, 1003
- Castelli F., Gratton R. G., Kurucz R. L., 1997, *A&A*, 318, 841
- Cayrel de Strobel G., Soubiran C., Friel E. D., Ralite N., Francois P., 1997, *A&AS*, 124, 299
- Cayrel de Strobel G., Soubiran C., Ralite N., 2001, *A&A*, 373, 159
- Chavez M., Malagnini M. L., Morossi C., 1997, *A&AS*, 126, 267
- Fioc M., Rocca-Volmerange B., 1997, *A&A*, 326, 950
- González Delgado R. M., Leitherer C., 1999, *ApJS*, 125, 479
- Hauschildt P. H., Allard F., Baron E., 1999a, *ApJ*, 512, 377
- Hauschildt P. H., Allard F., Ferguson J., Baron E., Alexander D. R., 1999b, *ApJ*, 525, 871
- Heiter U., Kupka F., van't Veer-Menneret C., Barban C., Weiss W. W., Goupil M.-J., Schmidt W., Katz D., Garrido R., 2002, *A&A*, 392, 619
- Katz D., Soubiran C., Cayrel R., Adda M., Cautain R., 1998, *A&A*, 338, 151
- Kauffmann G., Heckman T. M., Simon D. M. W., Charlot S., Tremonti C., Brinchmann J., Bruzual G., Peng E. W., and others, 2003, *MNRAS*, 341, 33
- Kupka F. G., Ryabchikova T. A., Piskunov N. E., Stempels H. C., Weiss W. W., 2000, *Baltic Astronomy*, 9, 590
- Kurucz R., 1992, in *IAU Symp. 149: The Stellar Populations of Galaxies*, p. 225
- Kurucz, R., 1993a, *ATLAS9 Stellar Atmosphere Programs and 2 km/s grid*. Kurucz CD-ROM No. 13. Cambridge, Mass.: Smithsonian Astrophysical Observatory, 1993., 13
- Kurucz, R., 1993b, *Diatomic Molecular Data for Opacity Calculations*. Kurucz CD-ROM No. 15. Cambridge, Mass.: Smithsonian Astrophysical Observatory, 1993., 15
- Kurucz, R., 1994, *Atomic data for opacity calculations*. Kurucz CD-ROM No. 1. Cambridge, Mass.: Smithsonian Astrophysical Observatory, 1994., 1
- Le Borgne J.-F., Bruzual G., Pelló R., Lançon A., Rocca-Volmerange B., Sanahuja B., Schaerer D., Soubiran C., Vílchez-Gómez R., 2003, *A&A*, 402, 433
- Lejeune T., Cuisinier F., Buser R., 1997, *A&AS*, 125, 229
- Lejeune T., Cuisinier F., Buser R., 1998, *A&AS*, 130, 65
- Lindgren L., Perryman M. A. C., 1996, *A&AS*, 116, 579
- Prugniel P., Soubiran C., 2001, *A&A*, 369, 1048
- Smalley B., Kupka F., 1997, *A&A*, 328, 349
- Smalley B., Gardiner R. B., Kupka F., Bessell M. S., 2002, *A&A*, 395, 601
- Steinmetz M., 2002, Munari U., ed., *GAIA Spectroscopy, Science and Technology*
- Stoughton C., Lupton R. H., Bernardi M., Blanton M. R., Burles S., Castander F. J., Connelly A. J., 2002, *Astronomical Journal*, 123, 485
- Straizys V., Liubertas R., Valiauga G., 1997, *Baltic Astronomy*, 6, 601
- Straizys V., Lazauskaite R., Valiauga G., 2002, *Baltic Astronomy*, 11, 341
- Worthey G., Faber S. M., Gonzalez J. J., Burstein D., 1994, *ApJS*, 94, 687
- Zwitter T., Munari U., Castelli F., 2002, in Munari U., ed., *GAIA Spectroscopy, Science and Technology*